LiDAR-Based 3D Reconstruction for Robotic Pipelines Inspection

Monika Sara Kawka[1], Lazaros Grammatikopoulos[1,2], Ilias Kalisperakis[1] and Christos Stentoumis[1]
[1]*up2metric, Michail Mela 21, Athens, Greece*
[2]*Department of Surveying and Geoinformatics Engineering, University of West Attica, Agiou Spiridonos 28, Egaleo, Greece*

Keywords: Robotics, LiDAR, Pipe Inspection, Computer Vision.

Abstract: Robotic platforms have transformed pipe inspection from routine checks into an automatic data-driven process. Such robotic systems often integrate computer vision technology to collect and analyze inspection data in an automated and efficient way and offer additional capabilities such as 3D reconstruction of pipes and precise measurement of deformations (e.g., dents, buckling). This work presents an initial case study of a robotic inspection system equipped with LiDAR and camera sensors capable of performing automatic pipeline inspections. This proof-of-concept study is dedicated to the 3D reconstruction of the pipeline using LiDAR data collected during inspections. Reconstruction accuracy is evaluated by computing the RMSE for pipe surface reconstruction and the deviation from the reference diameter of a single pipe in a controlled laboratory setting. Reconstruction results reach an accuracy higher than 2cm based on computed RMSE and a precision higher than 0.5cm in pipe diameter estimation. The current implementation is limited to the inspection of matte and non-reflective pipes. Still, it offers a straightforward and scalable solution for various industrial sectors. Future work will incorporate camera data to integrate color mapping into the 3D reconstruction model and detect potential defects and deformations in a pipe.

1 INTRODUCTION

Robotic platforms are widely adopted, at least in the research community, as an automated alternative to traditional pipe exploration. Robust inspection requires developing a robot that can adapt to various pipe conditions and diameters, which remains an active area of investigation (Kazeminasab et al., 2020; Zhao et al., 2020; Ab Rashid et al., 2020; Elankavi et al., 2022; Baballe et al., 2022). For the scope of this work, such a robotic platform was developed; however, in this contribution, emphasis is given on sensors' data fusion, the methodology employed for 3D reconstruction of pipelines in the form of point clouds and estimating the actual diameter of pipes, rather than on robot integration.

Visual information can enhance the automated pipe inspection process and facilitate quick and direct identification of the pipe's interior features. In (Kakogawa et al., 2019) a camera-equipped pipe inspection robot is used to perform shadow-based autonomous navigation in straight and winding pipe. In (Gunatilake et al., 2021) two IR cameras are used for stereo vision processing and reconstruction and one RGB camera to map the color information to the reconstructed 3D points. In (Tian et al., 2023), the visual information provided by a monocular camera is essential for the presented RGB-D SLAM algorithm. Others, exploit visual data to generate a digital twin using the Structure from Motion (SfM) algorithm (Summan et al., 2018; Kannala et al., 2008).

The highly symmetrical cylindrical shape of pipes is challenging to capture entirely with a conventional camera. Hence, to overcome the limitation of a narrow view visual sensor, cameras with wide-angle lenses are selected to collect data of the entire interior surface of the pipe. Most approaches use fisheye lens cameras (Tian et al., 2023; Summan et al., 2018; Kannala et al., 2008) or omnidirectional cameras (Matsui et al., 2010; Karkoub et al., 2021) to inspect pipes effectively.

Camera calibration is an essential step before the inspection process to ensure the accuracy of the collected data, especially when using a wide-angle camera lens. Camera calibration is usually performed using a planar calibration object, like a checkerboard or a grid of circles. Various techniques, camera models, and tools are available for the calibration process. In (Summan et al., 2018) the OCamCalib Toolbox is applied (Scaramuzza et al., 2006) for the calibra-

Kawka, M. S., Grammatikopoulos, L., Kalisperakis, I. and Stentoumis, C.
LiDAR-Based 3D Reconstruction for Robotic Pipelines Inspection.
DOI: 10.5220/0013390900003935
In *Proceedings of the 11th International Conference on Geographical Information Systems Theory, Applications and Management (GISTAM 2025)*, pages 195-202
ISBN: 978-989-758-741-2; ISSN: 2184-500X

tion of omnidirectional cameras, while in (Kannala et al., 2008) the generic camera model (Kannala and Brandt, 2006) is adopted for their fisheye lens cameras. The Matlab Calibration Toolbox[1] is used by (Hansen et al., 2011) to undistort the collected image data and the CamOdoCal (Heng et al., 2013) method is used by (Tian et al., 2023) to conduct intrinsics calibration.

Visual sensors are indeed valuable, since they provide a quick view of the pipes surface during inspection. However, the quality of the inspections depends highly, on the camera resolution and on lighting conditions. Therefore, robotic platforms for pipe inspection, often integrate laser technology, which is proven to significantly benefit the inspection process. LiDAR data, allow the detection of existing deformations that might not be visible through the camera data and are suitable for accurate geometric recording of the internal surface of pipelines. In (Gunatilake et al., 2021) 3D laser profiling is implemented, to generate 3D RGB-Depth maps, utilizing an IR laser beam with RGB and IR cameras. In (Matsui et al., 2010) an omnidirectional laser with an omnidirectional camera are combined to ensure full pipe coverage. Data from both omnidirectional sensors are used to reconstruct the pipe, by means of a light section method and SfM analysis. In the work of (Sepulveda-Valdez et al., 2023; Sepulveda-Valdez et al., 2024) a Technical Vision System (TVS) is employed, as a measuring tool to generate a complete point cloud of the pipe's interior. Another commonly used laser technology in pipe inspection is the Light Detection and Ranging (LiDAR) sensor. In (Tian et al., 2023), LiDAR-based constraints, derived from the pipes' underlying geometry, are combined with the proposed SLAM method to reduce long-term odometry drift. The method presented in (Zhao et al., 2023) improves the detection process in the inspection system by using a LiDAR system which is based on non-repetitive technology and an Inertial Measurement Unit (IMU). In (Moein and Himan, 2022) an automated framework is presented, that uses LiDAR data to identify the pipes' diameter and deflection.

In addition to using laser technologies for pipe surface reconstruction, the estimation of the pipe's diameter is widely adopted as a metric for the evaluation of the effectiveness of pipe surface reconstructions, for the estimation of the reconstructed surface's accuracy, but also for detecting possible deformations. In (Matsui et al., 2010) cylinder fitting is employed to measure the pipe's diameter. In contrast, (Sepulveda-Valdez et al., 2024; Moein and Himan, 2022) utilize circle fitting to find the diameter of the pipe. The k-nearest neighbors algorithm is also proposed for the same purpose (Moein and Himan, 2022).

This work represents a subset of the broader LASER4TWIN project, supported by the EU-funded initiative PIMAP4SUSTAINABILITY[2]. It introduces an initial case study of a robotic inspection system equipped with LiDAR and camera sensors for automated pipeline inspections. Specifically, it focuses on methodologies developed for data pre-processing, calibration, two-step registration method for the 3D reconstruction of a pipe, and its diameter estimation via cylinder fitting. For the evaluation of the 3D reconstruction method, the accuracy provided by RMSE is computed by measuring the average deviation between the observed 3D points and the approximated cylindrical surface. A confidence interval is employed to assess the precision of the estimated diameter.

2 METHODOLOGY

This section describes the approach adopted to develop the robotic inspection system. A short outline of the robotic platform is given in subsection 2.1. Subsection 2.2 covers the selected LiDAR and camera sensors, 2.3 discusses the calibration procedures adopted to ensure the optimal sensors fusion, and 2.4 focuses on the data collection process. In subsection 2.5, the pre-processing of point cloud data is addressed. Subsection 2.6 explains the two-step registration method using the Iterative Closest Point (ICP) algorithm. Finally, subsection 2.7 focuses on pipe diameter estimation.

2.1 Robotic Platform

In LASER4TWIN project, a custom robotic platform was designed and built by CIS Robotics[3] to meet the inspection system requirements. The robot has six-wheeled arms, providing enhanced stability and manoeuvrability within pipelines. It features DC motors integrated with wheel encoders and IMU. The IMU measurements are aligned with the robot's axes to ensure precise odometry data for accurate inspection. The robot's arms were designed to accommodate a range of pipe diameters from 30 cm to 45 cm. Notably, the range limitation of 30 cm to 45 cm applies specifically to the robot's arm design and does not reflect the constraints of the sensors. The LiDAR and

[1] mathworks.com/help/vision/ref/cameracalibrator-app.html

[2] https://pimap4sustainability2023.b2match.io/

[3] https://www.cis-robotics.com/, Av. Mar Cantábrico 17, Gijón-Asturias

camera sensors are placed at the front of the robot to enable data acquisition, along with two arc-shaped LED light arrays of 30 NeoPixels.

2.2 LiDAR and Camera Sensors

This section describes the selection of the LiDAR sensor and the digital cameras of the proposed inspection system. The MID-70 LiDAR was selected, due to its circular field of view, which was considered essential for scanning the pipe's interior. It uses a non-repetitive laser pattern and its compact size and small blind zone allow for adaptability in confined spaces.

The primary camera selected for the inspection system is the XIMEA MC050CG-SY, a 5 MP RGB camera with a Sony CMOS Pregius™ sensor and a USB 3.1 interface. It is paired with the Theia MY125M lens, an ultra-wide lens that reduces distortion using linear optical technology. The Theia MY125M lens was specifically chosen for its wide field of view, which maximizes the pipe's interior coverage. In addition, a 2 MP 1080p USB camera with a fisheye lens and IMX322 sensor was also integrated into the robot, for backup and future use. This camera was not actively used in the inspection process despite its integration.

2.3 Calibration

The camera-LiDAR fusion, adopted in the proposed platform, ensures a robust inspection system. LiDAR is used to effectively capture the geometry of the pipelines, while cameras capture RGB data to color the derived point cloud but also to allow visual inspection of the pipelines (identifying obstacles, defects etc.). To get optimal results, but also to allow the localization of objects detected in the camera feed, precise calibration of all sensors is required before executing an inspection mission. Therefore, as a first step, the camera calibration was performed using the Matlab Calibration Toolbox (Bouguet, 2023).

Next, a camera-LiDAR calibration algorithm was implemented in MATLAB. It is based on the method developed by the research team in the context of a mobile mapping platform (Grammatikopoulos et al., 2022). This algorithm uses a simple calibration planar board consisting of two crossing retroreflective stripes and an AprilTag at the intersection of the stripes. First, the four corners of AprilTag are used to detect the 2D position of the center of the marker on each image. Corresponding 3D LiDAR points are detected by estimating the center of two crossing retroreflective stripes (Figure1). Finally, based on established 2D to 3D point correspondences, the algorithm estimates a rigid transformation of the camera system relative to the Lidar frame (Grammatikopoulos et al., 2022). This transformation is introduced to the software tool described in Subsection 2.4, which synchronizes the robot's sensors.

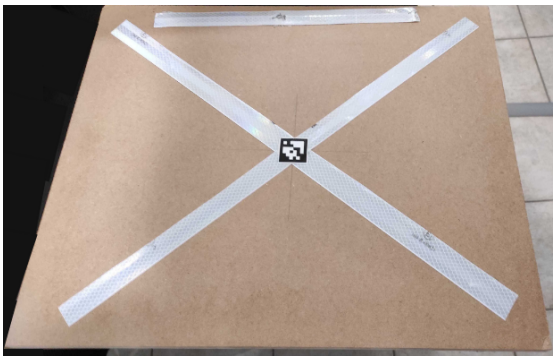

Figure 1: Calibration board consisting of two crossing retroreflective stripes and an AprilTag.

2.4 Data Collection

A software tool for data collection and synchronization was developed using the Robot Operating System (ROS)[4]. A Graphical User Interface (GUI) was implemented to allow users to initiate the data collection process. Once initialized, the cameras, the LiDAR sensor, and the other sensors and encoders of the robot publish data in different channels, while the implemented algorithm synchronizes the incoming data from all sources. Finally, the collected data are recorded and saved as a ROS Bag file.

2.5 Point Cloud Pre-Processing

Once a data collection mission is performed by the robot, the synchronized data are extracted from the ROS Bag and converted into more adequate formats for further processing, which are fed to the two-step registration process.

The raw point clouds recorded and collected by the LiDAR sensor often contain noise that should be removed to ensure accurate 3D reconstruction. As a pre-processing step, only low-noise points that belong to the pipe surface are retained 2. Firstly, the points with low confidence based on a relevant `Tag` value provided by the LiDAR manufacturer are rejected. The LiDAR has a blind zone of up to 5 cm and a circular field of view (70.4 degrees). Based on the range of the pipe's diameters (30cm-45cm), LiDAR can scan the first points of the pipe's surface at a distance of 21cm to 32 cm from it (3). However,

[4]https://ros.org/

the first measurements are prone to errors and present high noise levels (2). Therefore, it was decided to reject points closer than a certain distance (1 meter in the test missions). Finally, to further increase reliability, statistical filtering that removes any remaining points with noise levels exceeding 3σ is added.

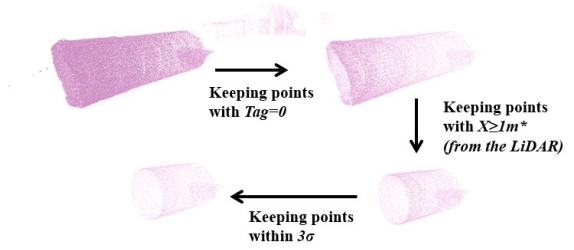

Figure 2: Pre-processing steps are applied to each scan to remove inaccurate data.

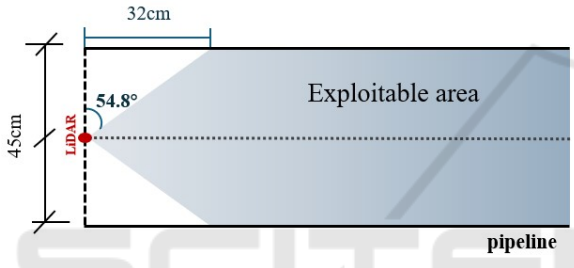

Figure 3: For a 45 cm diameter pipe, LiDAR can scan the first points of its surface at a distance of 32 cm from its current position.

2.6 3D Reconstruction via Two-Step Registration

Due to a pipe's cylindrical shape, ICP registration of consecutive point clouds in linear parts of a pipe becomes an ill-posed problem, as it is not possible to accurately estimate all six degrees of freedom (DOF) without additional constraints. Specifically, translation along the cylinder's axis and rotation around this axis cannot be determined without additional information about the robot movement. To address this issue, external data, such as odometry, is required to estimate the complete rigid body transformation.

In this work, the individual collected point clouds are merged using a two-step process based on the Iterative Closest Point (ICP) registration method, and data from the robot encoders to perform a 3D reconstruction of the pipeline. Initially, the ICP algorithm aligns two consecutive point clouds in each iteration by estimating a rigid-body transformation between them using a point-to-plane ICP approach (Chen and Medioni, 1992; Rusinkiewicz and Levoy, 2001). These transformations are then expressed in the coordinate system of the first point cloud to ensure the global alignment of all consecutive point clouds. This step is referred to as *local-to-global registration*. After the first *local-to-global registration*,

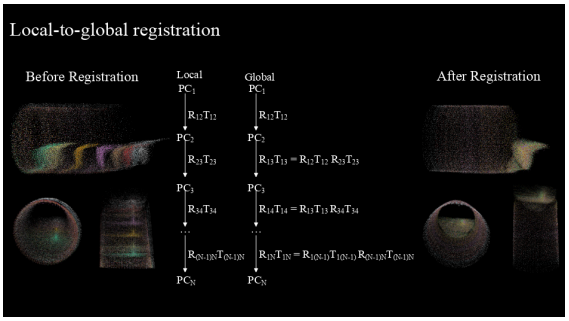

Figure 4: *Local-to-global registration*: the ICP algorithm aligns two consecutive point clouds in each iteration by estimating a rigid-body transformation between them using a point-to-plane ICP approach algorithm. These transformations are expressed in the coordinate system of the first point cloud to ensure the global alignment of all consecutive point clouds.

the difference between the encoder-provided transformation, which provides the necessary information about robot's movement, and the current ICP-estimated transformation, is calculated and used as the new initial transformation for the next *local-to-global registration*. A lower threshold is then applied for the final *local-to-global registration*, allowing the algorithm to integrate the absolute motion data from the encoders and the geometric constraints of the registered point clouds.

2.7 Pipe Diameter Estimation

The diameter of the 3D reconstruction model is estimated by fitting a cylinder surface. A cylinder fitting process is often employed in inspection systems for multiple tasks such as diameter estimation (Matsui et al., 2010), optimization (Tian et al., 2023), sectioned fitting (Kannala et al., 2008), or establishing a coordinate frame (Summan et al., 2018). The cylinder is defined by:

- $\mathbf{P}_0 = \begin{bmatrix} X_0 & Y_0 & Z_0 \end{bmatrix}^T$: A point on the cylinder's central axis,
- $\mathbf{P}_i = \begin{bmatrix} X_i & Y_i & Z_i \end{bmatrix}^T$: A point on the surface of the cylinder, and
- $\mathbf{d} = \begin{bmatrix} \cos(\phi)\cos(\theta) & \cos(\phi)\sin(\theta) & \sin(\phi) \end{bmatrix}^T$: A cylinder's central axis defined by a direction vector. Here, ϕ is an elevation angle and θ is an azimuthal angle.

- S_i: Cylinder's radius, which is perpendicular from the surface point $\mathbf{P}_i$ to cylinder's axis (direction vector $\mathbf{d}$).

The above parameters form a triangle, where vector $\overrightarrow{\mathbf{P}_0\mathbf{P}_i}$ corresponds to the triangle's hypotenuse. The adjacent side of the triangle is the projection of $\overrightarrow{\mathbf{P}_0\mathbf{P}_i}$ onto the direction vector $\mathbf{d}$, which aligns with the axis of the cylinder. The opposite side of the triangle corresponds to the radius S of the cylinder, which can be seen as the shortest distance from the point $\mathbf{P}_i$ to the line through $\mathbf{P}_0$ with direction vector $\mathbf{d}$.

The robot moves along the X-axis. Thus, $\mathbf{P}_0$ can be simplified and assumed to be located at $\mathbf{P}_0 = \begin{bmatrix} X_0 = 0 & Y_0 & Z_0 \end{bmatrix}^T$. Similarly, since the robot's moving axis approximately corresponds to the cylinder's axis, the initial values of Y_0, Z_0, ϕ, and θ are set to zero for simplicity. The radius S_i is calculated using the cross-product of $\overrightarrow{\mathbf{P}_0\mathbf{P}_i}$ and the direction vector $\mathbf{d}$, as shown in the equation below:

$$S_i = \frac{\|(\mathbf{P}_i - \mathbf{P}_0) \times \mathbf{d}\|}{\|\mathbf{d}\|} \tag{1}$$

The error $e_i = S_i - R$ measures how far a point $\mathbf{P}_i$ deviates from the cylinder's surface, where radius R is defined as half of the nominal pipe's diameter.

Levenberg-Marquardt algorithm (Moré, 1978) is used to minimize the error function $\sum_{i=1}^{n} e_i^2$, where n are multiple points sampled from the simplified surface of the reconstructed pipeline. The optimization parameters are:

$$\mathbf{x} = \begin{bmatrix} Y_0, Z_0, R, \phi, \theta \end{bmatrix}^T \tag{2}$$

Thus, the optimization problem can be defined as:

$$\min_{\mathbf{x}} E(\mathbf{x}) \tag{3}$$

Finally, the optimized radius can be converted to the diameter. Note that a pipe can be modelled as a perfect cylinder with a consistent diameter along its length because of its cylindrical shape and the assumption that it is straight. This assumption is crucial, as it allows the diameter estimation without accounting for any variations in curvature that would arise in a non-straight pipe.

3 RESULTS AND EVALUATION

Before executing an inspection mission, a camera-LiDAR calibration was performed to assure optimal results and provide the camera-LiDAR transformation to the ROS integration tool. A checkerboard selected for the calibration had seven rows and ten columns; its cell size was 25 mm. The robot with an integrated camera and LiDAR sensors was kept fixed while the checkerboard was moved and rotated for every subsequent image. A total of 25 images were taken for camera calibration purpose. The camera calibration process allowed for the estimation of the camera's interior orientation, which is essential for subsequent estimation of the relative position and orientation of the camera with respect to the LiDAR sensor. The camera intrinsics are given in Table 1 together with their estimation errors.

Table 1: Camera Intrinsics.

Camera Parameter	Computed Value	Estimation Error
Focal Length		
c_x (pixel)	370.46	±0.36
c_x (pixel)	370.97	±0.35
Principal Point		
x_o (pixel)	1221.11	±0.11
y_o (pixel)	1057.92	±0.13
Radial Distortion		
k_1	0.013138	±0.000222
k_2	-0.008703	±0.000117
k_3	0.000747	±0.000017
Tangential Distortion		
p_1	0.000436	±0.000050
p_2	0.000965	±0.000050
Mean Reprojection Error		
σ_o (pixel)	0.29	

Table 2: Camera-LiDAR Calibration Results.

Rigid transformation Parameters	Computed Value
Translation	
ΔX (cm)	3.53
ΔY (cm)	-0.76
ΔZ (cm)	5.92
Orientation	
ω (deg)	-34.76
ϕ (deg)	87.58
κ (deg)	-53.57
Mean Reprojection Error	
σ_o (pixel)	1.48

Next, to estimate a rigid transformation of the camera system relative to the LiDAR frame, the camera-LiDAR calibration described in 2.3 was applied using a simple calibration object consisting of two crossing retroreflective stripes and an AprilTag in their intersection. A total of 29 images and point clouds were captured simultaneously. Table 2 presents the camera-LiDAR calibration results.

To verify the effectiveness and reliability of the proposed inspection system, tests were performed in a controlled laboratory environment. For these tests, a polished steel pipe with a diameter of 45 cm and a length of approximately 2.5 meters (Figure 5) was

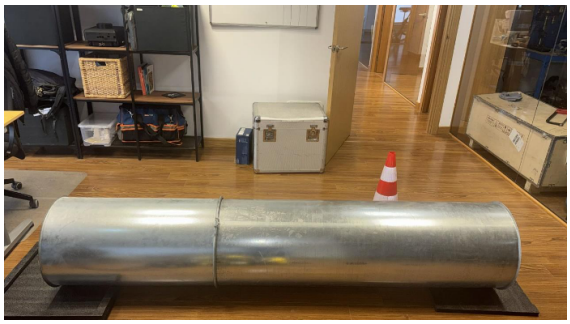

Figure 5: Polished steel pipe.

used.

During the early stages of testing, a challenge with LiDAR producing noisy data was encountered, as a result of the highly reflective nature of the polished surface material. This challenge was addressed by applying a matte white spray to the pipe's interior. This solution effectively minimized reflectivity and allowed the LiDAR to capture accurate data. It is important to note that this adjustment was specific to the reflective properties of polished surfaces, and the system can perform optimally without surface modifications in less reflective environments such as PVC, HDPE, clay or plastic pipes.

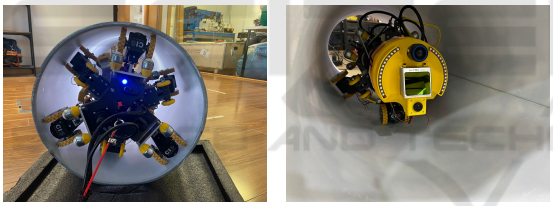

Figure 6: Robot platform inside the pipe.

To showcase the effectiveness of the proposed two-step registration method outlined in 2.6, firstly, 3D reconstruction was performed using only the provided odometry measurements from the robot encoders. Due to the noise in the data of the robot's IMU sensors, it was determined that an accurate 3D reconstruction could not be performed without further optimization, such as the proposed ICP registration. As detailed in 2.6, the *local-to-global* registration effectively addresses this challenge. The comparison presented in Figure 9 highlights the effectiveness of the proposed approach.

After completing the two-step registration, the pipe's diameter was calculated. Table 3 summarizes the pipe diameter estimation method results. The estimated pipe diameter was 45.431 cm, which closely matches the nominal pipe diameter of 45 cm.

Root Mean Square Error (RMSE) was calculated to evaluate the accuracy of the 3D reconstruction method. It measures the average deviation between

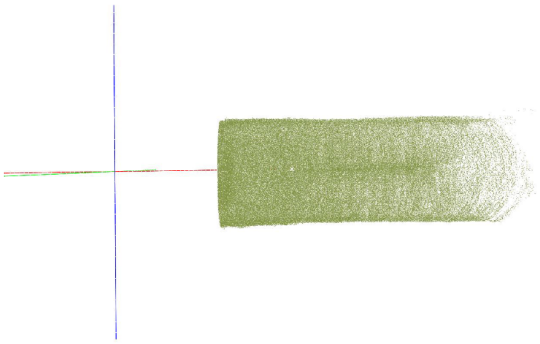

Figure 7: 3D reconstruction model using only odometry data.

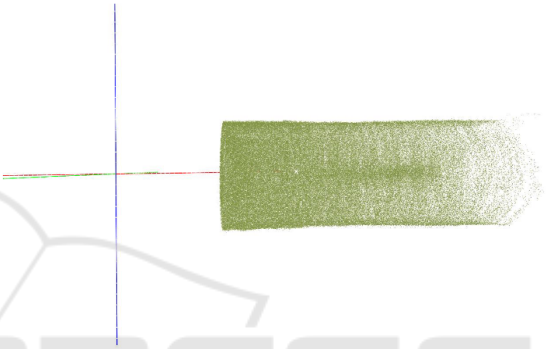

Figure 8: 3D reconstruction model using the proposed two-step registration method.

the observed 3D points of the 3D reconstruction model and the approximated cylindrical surface.

$$\sigma_o = \sqrt{\frac{1}{n-5}\sum_{i=1}^{n}(S_i - R)^2} \tag{4}$$

The precision of the estimated pipe's diameter is assessed by calculating the confidence interval, expressed as the two standard deviations of twice the optimized radius, indicating a 95% confidence level. Estimation error of all optimized parameters in Table 3 except radius and diameter corresponds to one standard deviation.

Table 3: Results of the pipe diameter estimation.

Optimization parameters	Computed Value	Estimation Error
Optimized Yo (m)	-0.059	±0.003
Optimized Zo (m)	-0.016	±0.003
Optimized R (cm)	22.715	±0.032
Optimized ϕ (deg)	0.469	±0.281
Optimized θ (deg)	-7.030	±0.279
Diameter (cm)	45.431	±0.064 (precision)
σ_o (cm)	0.48 (RMSE)	

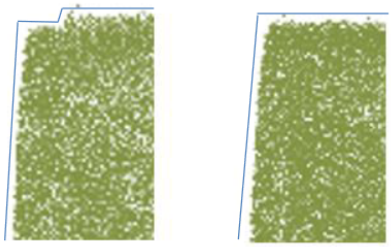

(a) Comparison between the 3D reconstruction model created using only odometry data (left image, Figure 7) and the 3D reconstruction model generated using the proposed method (right image, Figure 8)

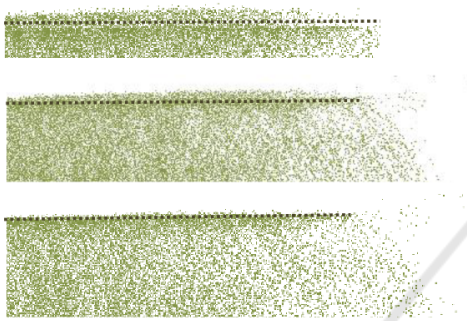

(b) Comparison of the registration process using raw data (top image), using only odometry measurements (middle image, Figure 7), and using the proposed two-step method (bottom image, Figure 8).

Figure 9: Comparison of the registration processes.

4 CONCLUSIONS

This work developed and evaluated a preliminary implementation of a robotic inspection system for non-reflective pipelines. The robotic system features six-wheeled arms, which enhance stability and adaptability for pipeline diameters ranging from 30 cm to 45 cm. Combining the MID-70 LiDAR and the XIMEA camera enables wide coverage and high-resolution data acquisition. Using accurate calibration of LiDAR and camera sensors, it allows 3D reconstruction via a two-step registration method. Evaluation results validate the proof-of-concept, demonstrating the system's efficiency by achieving a precision higher than 0.5 cm in diameter estimation and accuracy higher than 2cm in 3D reconstruction.

This study presents a pilot implementation and is not without limitations. First, the robot must be redesigned to inspect pipes with diameters larger than 45cm. Although the camera is integrated and ready to be used in the robot platform, its usage is not presented in this initial study. Experiments are conducted only in a controlled laboratory environment with a single pipe type, and real-world scenarios with varying pipe materials, diameters, and environmental conditions should be explored. Finally, this initial case study lacks a comparison analysis of the proposed method with other state-of-the-art systems.

Future improvements will focus on leveraging camera data to integrate color mapping into a 3D reconstruction method and allow visual inspection of the pipelines (identifying obstacles, defects, etc.). Moreover, a robot platform will be redesigned to refine the system for diverse pipeline materials and diameters. Two-step registration and diameter estimation methods will also be refined to handle more challenging pipes with non-constant diameters. Finally, a refined robotic system will be benchmarked to identify its potential limitations, validate its robustness, and demonstrate its practical usability in real-world pipeline inspection scenarios.

ACKNOWLEDGEMENTS

This work was part of LASER4TWIN project, supported by the European Union through the EU-funded project PIMAP4SUSTAINABILITY "Photonics for International Markets and Applications for Sustainability", in its Innovation Open Call. The authors would also like to express their gratitude to their partner in the LASER4TWIN project, CIS Robotics, particularly Christian J. Robledo and Adrián Álvarez García, for designing and manufacturing the robot and for integrating the developed technologies.

REFERENCES

Ab Rashid, M. Z., Mohd Yakub, M. F., Zaki bin Shaikh Salim, S. A., Mamat, N., Syed Mohd Putra, S. M., and Roslan, S. A. (2020). Modeling of the in-pipe inspection robot: A comprehensive review. *Ocean Engineering*, 203:107206.

Baballe, M. A., Bello, M. I., Hussaini, A., and Musa, U. S. (2022). Pipeline inspection robot monitoring system. *Journal of Advancement in Robotics*, 9(2):27–35.

Bouguet, J.-Y. (2023). Camera Calibration Toolbox for Matlab.

Chen, Y. and Medioni, G. (1992). Object modelling by registration of multiple range images. *Image and Vision Computing*, 10(3):145–155.

Elankavi, R. S., Dinakaran, D., Chetty, R. K., Ramya, M., and Samuel, D. H. (2022). A review on wheeled type in-pipe inspection robot. *International Journal of Mechanical Engineering and Robotics Research*, 11(10).

Grammatikopoulos, L., Papanagnou, A., Venianakis, A., Kalisperakis, I., and Stentoumis, C. (2022). An Ef-

fective Camera-to-Lidar Spatiotemporal Calibration Based on a Simple Calibration Target.

Gunatilake, A., Piyathilaka, L., Tran, A., Vishwanathan, V. K., Thiyagarajan, K., and Kodagoda, S. (2021). Stereo Vision Combined With Laser Profiling for Mapping of Pipeline Internal Defects. *IEEE Sensors Journal*, 21(10):11926–11934.

Hansen, P., Alismail, H., Rander, P., and Browning, B. (2011). Monocular visual odometry for robot localization in LNG pipes. In *2011 IEEE International Conference on Robotics and Automation*, pages 3111–3116. IEEE.

Heng, L., Li, B., and Pollefeys, M. (2013). CamOdoCal: Automatic intrinsic and extrinsic calibration of a rig with multiple generic cameras and odometry. In *2013 IEEE/RSJ International Conference on Intelligent Robots and Systems*, pages 1793–1800. IEEE.

Kakogawa, A., Komurasaki, Y., and Ma, S. (2019). Shadow-based operation assistant for a pipeline-inspection robot using a variance value of the image histogram. *Journal of Robotics and Mechatronics*, 31(6):772–780.

Kannala, J. and Brandt, S. S. (2006). A generic camera model and calibration method for conventional, wide-angle, and fish-eye lenses. *IEEE Transactions on Pattern Analysis and Machine Intelligence*, 28(8):1335–1340.

Kannala, J., Brandt, S. S., and Heikkilä, J. (2008). Measuring and modelling sewer pipes from video. *Machine Vision and Applications*, 19(2):73–83.

Karkoub, M., Bouhali, O., and Sheharyar, A. (2021). Gas pipeline inspection using autonomous robots with omni-directional cameras. *IEEE Sensors Journal*, 21(14):15544–15553.

Kazeminasab, S., Aghashahi, M., and Banks, M. K. (2020). Development of an inline robot for water quality monitoring. In *2020 5th International Conference on Robotics and Automation Engineering (ICRAE)*, pages 106–113.

Matsui, K., Yamashita, A., and Kaneko, T. (2010). 3-D shape measurement of pipe by range finder constructed with omni-directional laser and omni-directional camera. In *2010 IEEE International Conference on Robotics and Automation*, pages 2537–2542. IEEE.

Moein, E. and Himan, H. J. (2022). *Automated Condition Assessment of Sanitary Sewer Pipes Using LiDAR Inspection Data*, pages 136–144. Proceedings. American Society of Civil Engineers (ASCE).

Moré, J. J. (1978). The levenberg-marquardt algorithm: Implementation and theory. In Watson, G. A., editor, *Numerical Analysis*, pages 105–116, Berlin, Heidelberg. Springer Berlin Heidelberg.

Rusinkiewicz, S. and Levoy, M. (2001). Efficient variants of the ICP algorithm. In *Proceedings Third International Conference on 3-D Digital Imaging and Modeling*, pages 145–152. IEEE.

Scaramuzza, D., Martinelli, A., and Siegwart, R. (2006). A Toolbox for Easily Calibrating Omnidirectional Cameras. In *2006 IEEE/RSJ International Conference on Intelligent Robots and Systems*, pages 5695–5701. IEEE.

Sepulveda-Valdez, C., Sergiyenko, O., Alaniz-Plata, R., Núñez-López, J. A., Tyrsa, V., Flores-Fuentes, W., Rodriguez-Quiñonez, J. C., Mercorelli, P., Kolendovska, M., Kartashov, V., Miranda-Vega, J. E., and Murrieta-Rico, F. N. (2023). Laser Scanning Point Cloud Improvement by Implementation of RANSAC for Pipeline Inspection Application. In *IECON 2023-49th Annual Conference of the IEEE Industrial Electronics Society*, pages 1–6. IEEE.

Sepulveda-Valdez, C., Sergiyenko, O., Tyrsa, V., Mercorelli, P., Rodríguez-Quiñonez, J. C., Flores-Fuentes, W., Zhirabok, A., Alaniz-Plata, R., Núñez-López, J. A., Andrade-Collazo, H., Miranda-Vega, J. E., and Murrieta-Rico, F. N. (2024). Mathematical Modeling for Robot 3D Laser Scanning in Complete Darkness Environments to Advance Pipeline Inspection.

Summan, R., Jackson, W., Dobie, G., MacLeod, C., Mineo, C., West, G., Offin, D., Bolton, G., Marshall, S., and Lille, A. (2018). A novel visual pipework inspection system. *AIP Conference Proceedings*, 1949(1):220001.

Tian, T., Wang, L., Yan, X., Ruan, F., Aadityaa, G. J., Choset, H., and Li, L. (2023). Visual-Inertial-Laser-Lidar (VILL) SLAM: Real-Time Dense RGB-D Mapping for Pipe Environments. In *2023 IEEE/RSJ International Conference on Intelligent Robots and Systems (IROS)*, pages 1525–1531. IEEE.

Zhao, M., Fang, Z., Ding, N., Li, N., Su, T., and Qian, H. (2023). Quantitative Detection Technology for Geometric Deformation of Pipelines Based on LiDAR.

Zhao, W., Zhang, L., and Kim, J. (2020). Design and analysis of independently adjustable large in-pipe robot for long-distance pipeline. *Applied Sciences*, 10(10).